

A Measuring Instrument for Off-road Vehicle Performance Testing

Fan Yang¹, Guoyu Lin² and Weigong Zhang³

Master of Instrument and Meter Engineering, Southeast University
¹yfan0510@sina.cn; ²andrew.lin@seu.edu.cn; ³zhangwg1020@qq.com

Abstract

An overall description of a measuring instrument, wheel force transducer (WFT), developed for off-road vehicle performance testing is presented in the paper. For the research of off-road vehicle performance, it is important to determine the forces and torques as a response of the interaction between the wheel and the terrain. The WFT developed provides a solution of the direct measurement of the physical quantities. The WFT was designed as an automatic real-time data acquisition device with the wireless transmission technology. In the aspect of mechanical structure, only minor modifications of the wheel rim and two flanges were required for the installation of the WFT. The elastomeric of the sensor was designed with excellent mechanical strength for wheeled vehicles of weights ranging from 1.2 to 15 ton. Field tests were conducted after static calibration and dynamic calibration. The WFT was installed on the two front wheels of a 1.6-tone weight car. In preliminary field test, various vehicle maneuvers were executed for the validation of the validity, reliability and accuracy of the whole system, which was demonstrated by the test results. Six kinds of special testing pavements were selected to simulate the off-road situations. From the results, great potential of the WFT system is indicated in the application of off-road vehicle performance testing.

Keywords: *off-road vehicle performance, wheel force transducer, real-time data acquisition system, field test*

1. Introduction

With growing globalization of the economy, the vehicles are required to reach a wider range of areas from on-road to off-road. However, off-road situations bring a special range of challenges to the vehicles, military or civilian. The vehicle performance, such as trafficability, turnability, maneuverability and ride stability, is quite different from that on general road [1]. Since the terrains in off-road situations tend to be rough or soft. Especially, soft terrain means low cohesion and weak bearing ability, which has a great negative effect on vehicle's tractive ability and steering performance. Therefore, there is a great demand for a research of the dynamics of the vehicles to guarantee various characteristics during driving: general safety, ride comfort, reliability, stability, robustness, and off-road performance. For instance, C. Senatore and C. Sandu discussed an off-road model and predicted the longitudinal and lateral forces, then analyzed the torque distribution influence on tractive efficiency and mobility [2]. Zvi Shiller *et al.*, analyzed the dynamic stability of off-road vehicles with proposed vehicle models [3]. Jaroslaw Pytka did a research on the lateral dynamics of off-road vehicles by a field experiment, in which wheel forces were measured by wheel dynamometers [4]. Jaroslaw Pytka studied the effect of steering dynamics on lateral dynamics [5]. V. V. Vantsevich *et al.*, analyzed the optimized control of the wheel driving forces for off-road vehicle dynamics [6].

As we can see from the research mentioned above, for analyzing the dynamics, it is necessary to determine the dynamic forces and torques produced during the interaction between the soil and the wheels. As shown in Figure 1, the forces and torques include longitudinal force (F_x), vertical force (F_z), lateral force (F_y), heeling torque (M_x), twist torque (M_y) and aligning torque (M_z). These forces and torques are used as necessary input or output in the models mentioned. How to gain the dynamic forces and torques is a great issue.

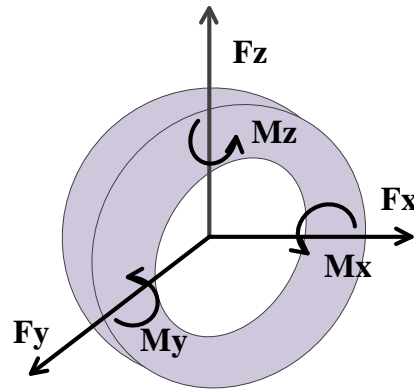


Figure 1. The Diagram of Six-Dimensional Forces of Wheel

Great efforts have been made to determine the forces and torques through various kinds of methods and models. For instance, in the research of off-road vehicle trafficability, a variety of models have been established to describe the interaction between the soil and the wheels, such as the semi-empirical model, the empirical model and the analytical model [7]. The semi-empirical model is pioneered by Bekker [8, 9] and later by Wong [10] to predict the tractive performance of vehicles. The prototype of the empirical model is put forward at the US Army Corps of Engineers, Waterways Experiment Station (WES) [11]. The empirical equations are produced from the comparison between the field data and the vehicle parameters. The analytical model is appealing and developed in recent years, such as finite element modes (FEM) [12] and discrete element models (DEM) [13]. It is a method of computer simulation to simulate the consequential forces and torques of the interaction. However, the predicting methods and models have some limitations and there are significant deviations between the predicting results and the actual.

The measurement through instruments can be used as a direct way to gain the forces and torques, which provides more direct and more accurate data. It is also a validation of the models for predicting. Similarly, for instance, in the research of off-road vehicle trafficability, soil-bin tests are widely used as a kind of model tests [14-16]. However, they cannot reflect all the characteristics in wheel-soil interactions, especially the dynamic characteristics as in real vehicle situations. So real vehicle test data is essential for further validation of the prediction models and can provide strong base data for the further research of off-road vehicle performance. By contrast, wheel force transducer is an important instrument to measure the forces and torques on real vehicles [17]. This kind of direct measuring instrument can be installed on the real vehicle without changes in the vehicle's structure. Only the wheel rim should be modified. Thus, the dynamic responses between the soil and the wheels can be recorded during field tests. For instance, a description of a rotating wheel dynamometer developed for off-road testing of military vehicles is presented [18], as shown in Figure 2(a). A new integrated testing system for the validation of stochastic vehicle-snow interaction models is introduced [19], in which the instrumented ground vehicle was equipped with the wheel force transducer (WFT) to measure the required wheel forces and torques as shown in Figure 2(b).

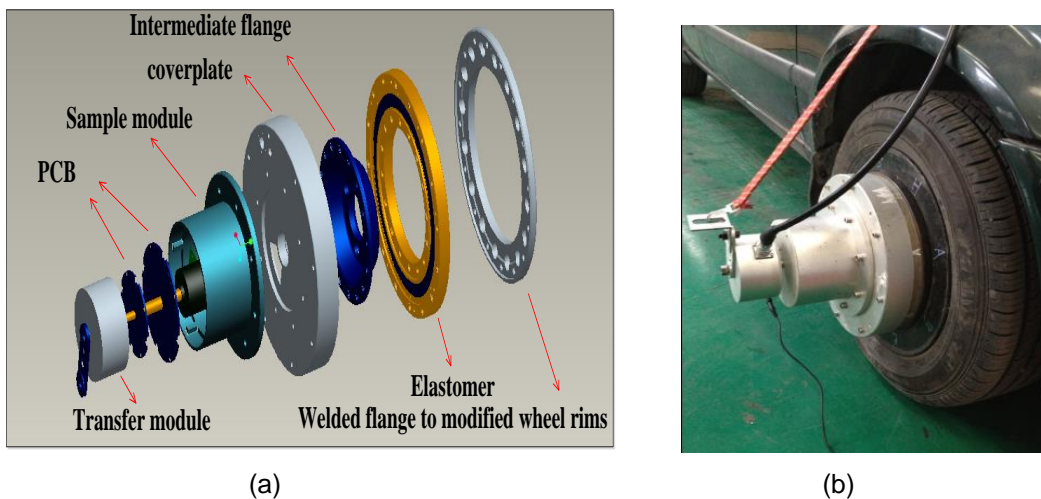


Figure 2. (A) Application of a Rotating Wheel Dynamometer (B) Application of Wheel Force Transducer

A number of wheel force transducers are currently commercially available, however, whose price is beyond the scientific research budget of university studies. Therefore, a wheel force transducer was designed and fabricated by Southeast University for off-road testing. This paper makes a description of the design, manufacture and calibration of the complete WFT system. The results of field tests are presented to demonstrate the effectiveness and capability of the testing system and show the potential of the system in the research of off-road vehicle performance testing.

2. The Overall Structure of WFT

As shown in Figure 3(a) and Figure 3(b), the WFT developed by Southeast University is composed of the following subsystems: the sensor (the elastomer, the electric bridge), the modified rims, the mounting parts (the flanges, the mounting screws), the automatic real-time data acquisition system (the sample module, the transfer module). Figure 3(c) is the electrical flowchart of the WFT. In the process of movement, the transfer module is static relative to the vehicle, and the other parts of the WFT rotate with the wheel. Each subsystem is described in detail below.



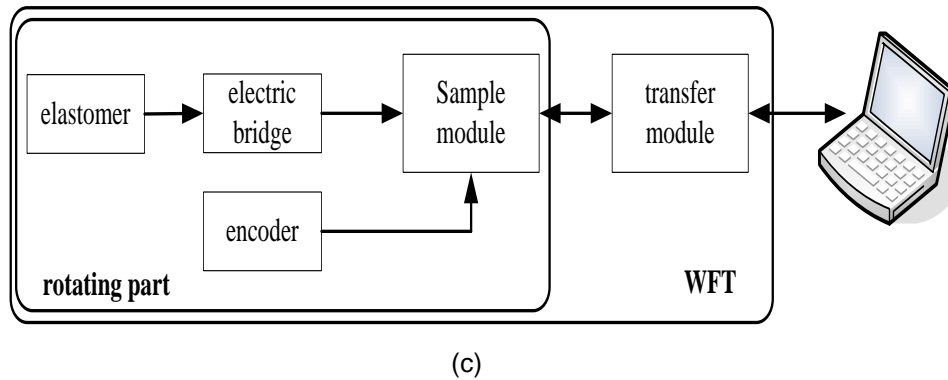


Figure 3. (A) The Assembly Diagram of WFT (B) A Picture of WFT (C) the Electrical Flowchart of WFT

2.1. The Sensor

The design of the elastomer is a key part of the WFT. The elastomer is sensitive to the forces and torques acted on the wheel through the caused deformation. The sensitivity of the elastomer should be guaranteed. As the elastomer is fixed on the rotating wheel, it suffers from poor working conditions in off-road situations. Hence, high requests are put forward to the structure and the installation of the elastomer. Finite element analysis was carried out for the demand of sensitivity and load carrying capacity. Firstly, 40CrNiMoA was chosen as the material of the elastomer. Secondly, the eight spoke structure was exploited, which has several advantages: small axial size, large radial force load capacity, and small impact on the whole vehicle. As shown in Figure 4(a), the elastic body consists of an inner ring, an outer ring, and eight elastic beams. The mounting holes on the inner ring and outer ring are used to connect the elastomer. 8 elastic beams are distributed uniformly between the inner ring and the outer ring. When various forces and torques are acted on the wheel, deformation of the elastic beam is caused. Resistance strain gauges were placed on the elastic beam to sense the deformation. The position of the resistance strain gauges was designed specially [20]. The measurement of the longitudinal force (F_x) is shown as an example. Resistance strain gauges R1-R4 were placed beside the elastic beams in couple as shown in Figure 4(a). Then the differential electric bridge of the resistance strain gauges was formed by the bridge circuit to eliminate the common-mode error and amplify the deformation of each single resistance strain gauge as shown in Figure 4(b). The wheel with the elastomer assembled on the real wheel is shown in Figure 4(c).

2.2. The Modified Wheel Rim

Only a small part of the original rim is needed to be modified to fit the installation of the WFT on the vehicle. Wheels of different diameters are modified in the same way. In the case of the prototype solution, the wheel rim was modified by cutting off the central part and then welding a special designed welded flange to the rim. The mounting holes on the weld flange will match the ones on the outer ring of the elastomer as shown in Figure 4(c).

2.3. The Mounting Parts

The mounting parts for the WFT are particularly important, because the forces and torques acted on the wheel hub are transmitted to the sensor by the mounting parts. The pretightening load introduced by the mounting screws may affect the precise measurement. Optimal scheme is put forward by computer simulation of finite element analysis. In this design, an intermediate flange was designed to connect the whole

integrated wheel to the wheel hub with 4 mounting screws as shown in Figure 4(c). While it was attached to the elastomer by means of sixteen M8 screws distributed uniformly in a circle, which contributes to the transmission of the forces. The screws were special customized with high loading capacity. On the other hand, the elastomer was attached to the modified rim by sixteen M8 screws ensuring the reliability during rotating in high speed and poor working conditions.

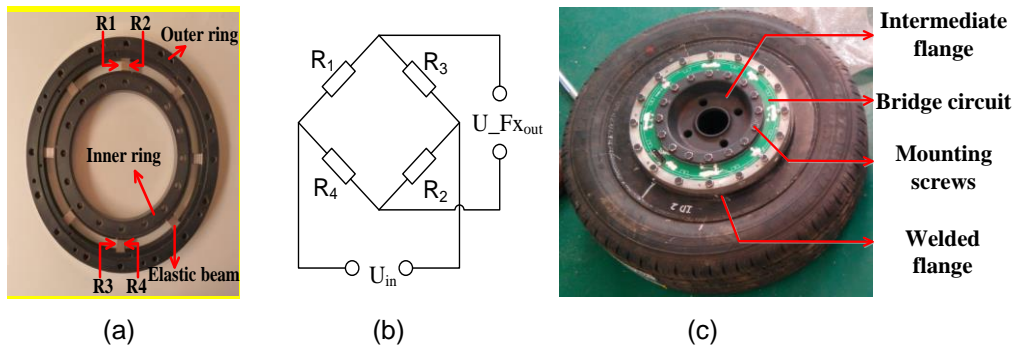


Figure 4. (A) The Elastomer with Resistance Strain Gauges (B) The Electric Bridges (C) Installation of the Elastomer

2.4. The Automatic Real-Time Data Acquisition System

The automatic real-time data acquisition system is another key part of the WFT. A well-designed data acquisition system can ensure the data to be transmitted accurately and fast. As the WFT is a rotating sensor, a special transfer method should be adopted. Two methods are widely used for the existing commercial wheel force transducers, rotating slip ring transducer and telemetry frequency system.

The rotating slip ring transducer is used as a way of wire transmission, which has distinct advantages, accurate and fast. However, there is some difficulty in the manufacture of the rotating slip ring transducer in domestic. And the cost of foreign import is too high. Owing to the development of wireless transmission technology, a method of wireless transmission technology is proposed as an optimal solution. The data acquisition system consists of two parts, the sample module and the transfer module. The main idea of it follows. The sample module is used to sample the wheel forces and rotation angle from the elastomer and the encoder. It connects to the elastic body by the coverplate over the elastomer and rotates with the rolling wheel. Then it sends the signals to the transfer module by wireless transfer module. The transfer module connects to the collection module by the bearing and does not rotate with the rolling wheel. Finally it can forward the data to the data recording device by CAN bus. This design approach of transmission makes it possible to transmit the data synchronously and real time, which contributes to on-line analysis and real-time control of the vehicle.

The electric block diagram of the sample module is shown in Figure 5. The sample module is powered by lithium battery pack. Differential voltage signal from the electric bridge is filtered and amplified here by the signal conditioner. Then the preliminary processed signal is sent to the A/D sampling channel of MCU. Meanwhile, the current angle signal from the encoder is sent to the I/O of MCU. Finally, the signals sampled are packaged for sending by wireless transfer module. The accuracy and reliability of the wireless transmission is tested for dozens of hours uninterruptedly both in laboratory and field environment. The result is ideal. The circuit board is shown in Figure 6.

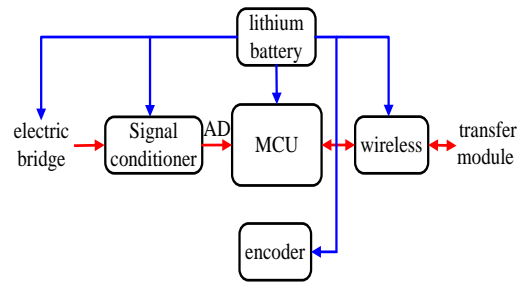


Figure 5. The Electric Block Diagram of the Sample Module

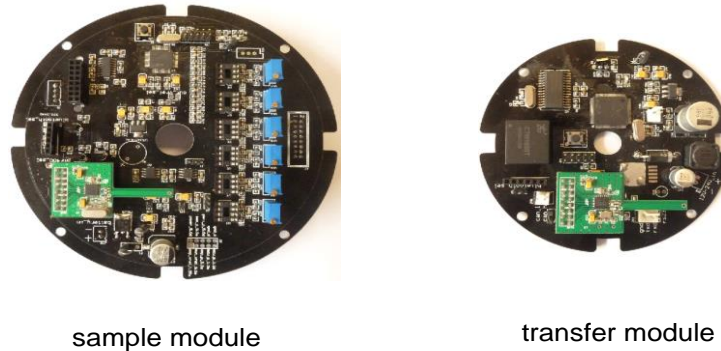


Figure 6. The Circuit Board

The electric block diagram of the transfer module is shown in Figure 7. It is powered by the power module of the data recording device. In fact, the transfer module plays a role of a bridge in the communication between the sample module and the data recording device. Firstly, it receives the wireless signals from the sample module. Then it sends the signals to the data recording devices by CAN bus. In the meantime, it transfers control commands and response signals between them. The circuit board is shown in Figure 6.

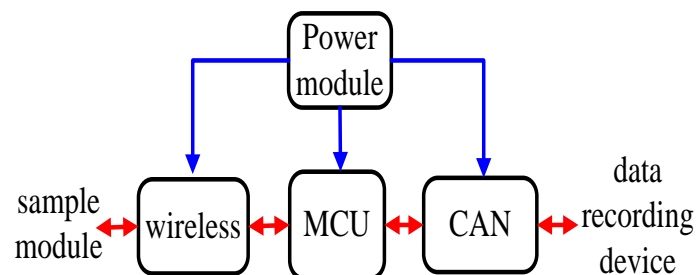


Figure 7. The Electric Block Diagram of the Transfer Module

3. Static Calibration

After the manufacture and installation of the WFT, static calibration is essential to make the measured raw data to fit the real situation. The basic idea of static calibration is to input the standard force on the sensor and record the output of it. Then the input and output of the sensor are processed and compared to gain the corresponding relation, the V-KN and V-KNm. As shown in Figure 8(a), the WFT was calibrated on a special-designed test stand, which has three hydraulic devices to simulate the input of the forces and torques. Owing to the special structure of the elastomer, the forces and torques were calibrated independent to each other. The tests were conducted for +/-20KN (Fx, Fz) and

for +/-2KN (F_y) loads with a step of 4 KN and 400 N. The torque channels were calibrated within a range of -2 to 2 KNm, with a step of 400 Nm. The input and output of every step were recorded. The procedure of the test was conducted repeatedly. The result of channel F_x is shown in Figure 8(b) as an example.

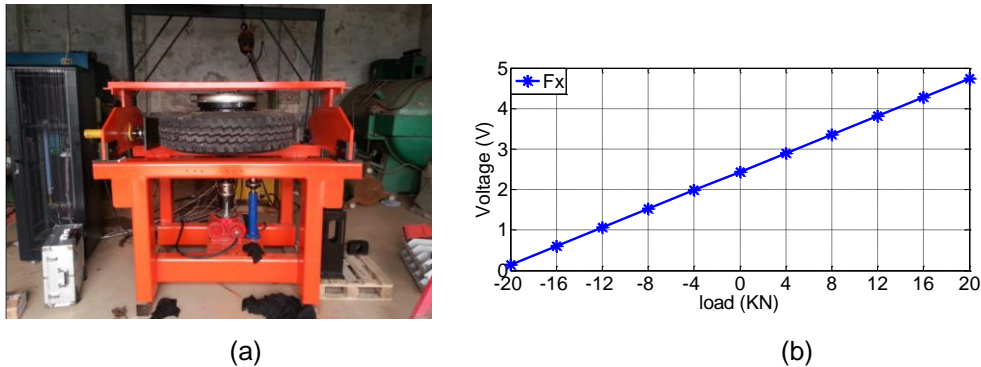


Figure 8. (A) A Special-Designed Test Stand for Calibration (B) Calibration of the FX Channel

4. Dynamic Calibration

Before the real vehicle field tests, a series of dynamic calibration tests were done on a road wheel testbed produced by MTS in 1986 to make an initial validation of the WFT data [21]. For security reasons, the test-bed cannot be displayed in public. So a similar device is shown in Figure 9(a) to indicate its primary function and principle. Figure 9(b) shows the structure of the dynamic calibration testbed. A is the driving wheel, applying the driving force and normal force to the driven wheel B. The WFT to be tested is installed on the wheel B. O1 is the rotating center of A, which is fixed in the beam H. The beam is controlled by a hydraulic cylinder and can move the driving wheel in the horizontal direction. Thus a normal force is added to B. A coordinate system is defined in Figure 9(b) to simulate the vehicle coordinate system. The values of F_x and F_z applied to B are measured by the sensors on the dynamic calibration testbed and displayed on the screen of the host computer. In such way, the measured values can be used as the true value to validate the accuracy of the WFT data. The comparison result of F_z is displayed as an example. In the experiments, the normal force applied to the driven wheel B was set to 10kN, 20kN, 28kN, 36kN and 26kN successively while the rotating speed was set to 4.2r/m, 8.6r/m and 4.3r/m. Fig. 10 shows the comparison result of F_z from the WFT and the dynamic calibration testbed. The errors (the maximum error, average error and error rate) are shown in Table 1. It is shown that the error rate ranges from 0.39% to 8.4%, which is acceptable and indicates a good effect of the WFT.

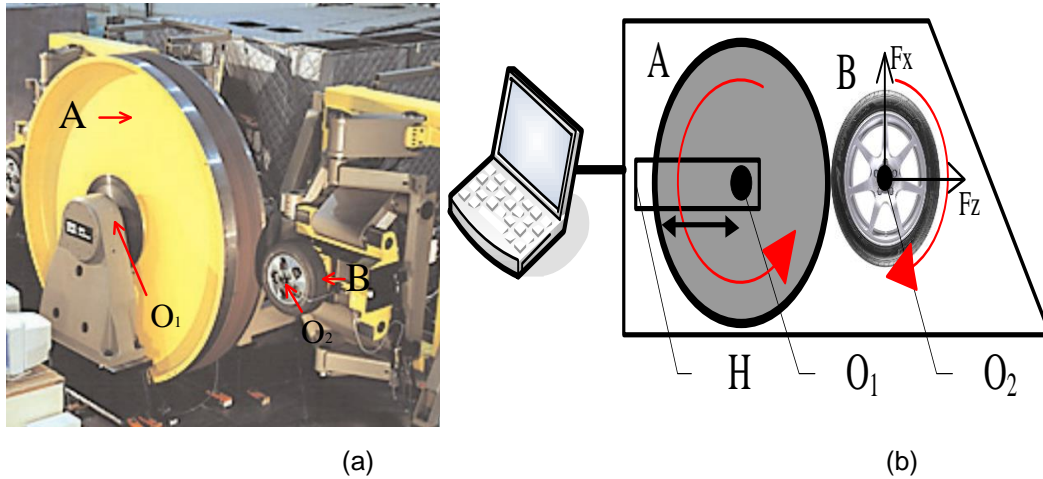


Figure 9. (A) MTS Road Wheel Test bed (B) The Structure of the Test bed

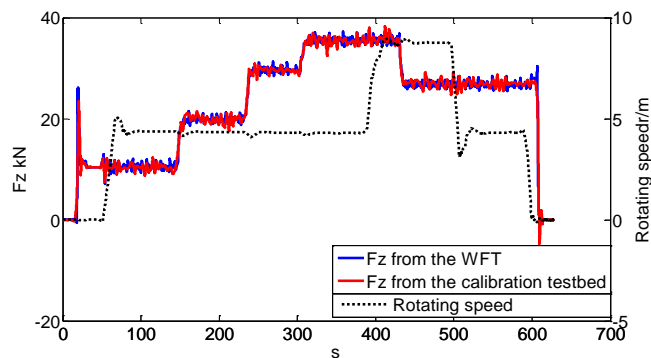


Figure 10. Comparison of Fz from the WFT and the Calibration Test bed

Table 1. Dynamic Error

Situation	Max error (kN)	Average error (kN)	Error rate (%)
0r/m(0~10kN)	2.15	0.84	8.4
4.2r/m(10kN)	1.56	0.45	4.5
4.2r/m(20kN)	0.47	-0.41	2.05
4.2r/m(28kN)	-1.89	0.78	2.79
4.2r/m(36kN)	1.24	0.36	1
8.6r/m(36kN)	1.63	-0.14	0.39
8.6r/m(26kN)	-0.87	-0.37	1.42
4.3r/m(26kN)	1.65	0.43	1.65
0r/m(26kN)	2.79	1.04	4
Whole	2.79	0.51	

5. Field Tests and Results

5.1. Preliminary Field Tests

A series of preliminary field tests were conducted to validate the effectiveness and accuracy of the whole system of the WFT. The system was applied to a conventional car, 1.6-tone weight. The WFT was installed on the two front wheels shown in Figure 11(a). Installation of the WFT was convenient. Only two persons and conventional tools were required. During the field test, the data acquisition system can be controlled by one technician. The preliminary tests were done on rigid roads because the response on typical road is already known to some extent, which contributes to the validation. Various vehicle maneuvers were executed, such as low-speed straight driving, straight accelerate-brake driving, driving around a large circle with constant speed and Figure-8 driving with constant speed. The routes of the preliminary test are shown in Figure 11(b). The test procedure is indicated by the direction of the arrow and the sequence number.

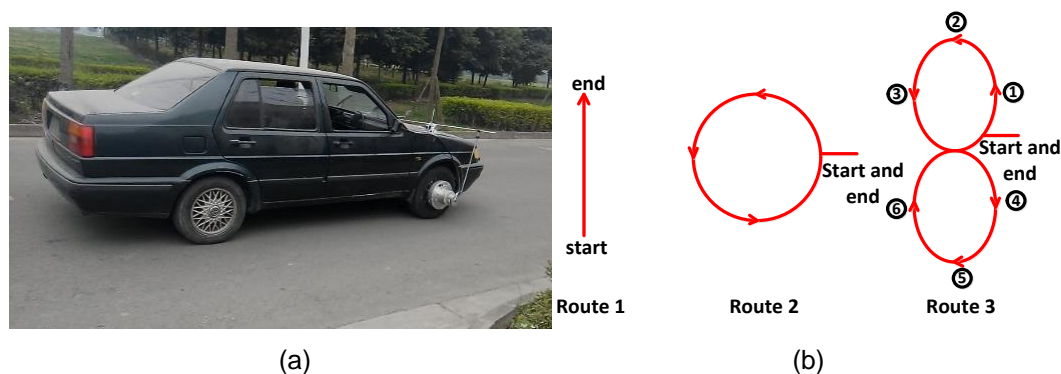


Figure 11. (A) The Instrumented Vehicle in the Field Test (B) The Routes of the Vehicle Maneuvers

The testing data for the results was selected from the straight accelerate-brake driving, circle driving and figure-8 driving. Wavelet filter was used here to reduce the high frequency noise in the raw data, while the Savitzky-Golay method was used to smooth the data curve.

In the field test of straight accelerate-brake driving, vehicle's gear was kept on the first gear from beginning to end, while the vehicle accelerator was stepped down slowly until the velocity gains to a certain level about 35km/h. Finally an emergency braking was taken. The whole process was repeated several times. Figure 12(a) shows the longitudinal force (F_x) called the drawbar pull and the driving torque (M_y) as a function of time. When the vehicle is accelerating, the drawbar pull keeps positive and changes with the depth of the vehicle accelerator. Then it decreases sharply to negative value when braking, in accordance with the test process. As we can see, the shape of the two curves is similar, which corresponds to reality. The difference between the traction force produced by driving torque (M_y) and the drawbar pull (F_x) defines the value of the total motion resistance. Figure 12(b) shows the vertical force (F_z) and the driving torque (M_y) as a function of time. As the static weight of each front wheel is about 400 kilos, F_z ranges from 3KN to 4.7KN as a dynamic response of the vehicle. When braking, F_z increases sharply. Then Figure 12(c) shows the wheel speed (V) and the driving torque (M_y) as a function of time. The shape of the speed curve validates the process of the accelerate-brake driving. When the driving torque (M_y) can overcome the motion resistance, the vehicle is in the stage of accelerating. On the contrary, when the driving torque decreases, even to negative, the vehicle is taking a braking.

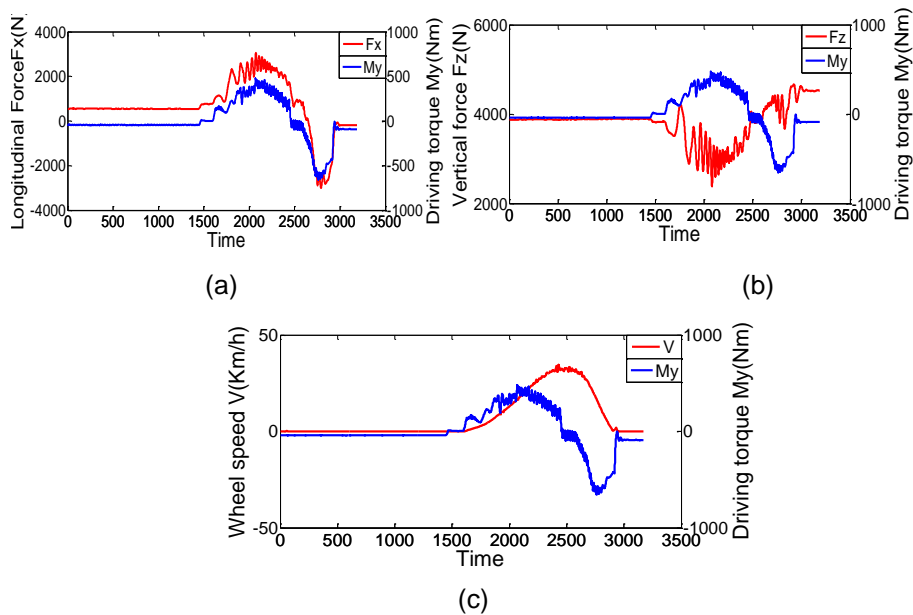
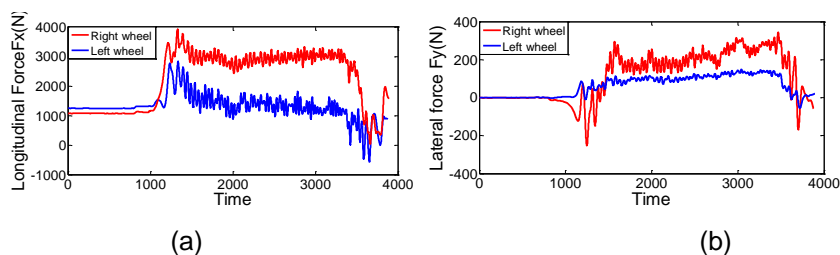


Figure 12. (A) Traction Torque and Drawbar Pull as a Function of Time (B) Traction Torque and Vertical Load as a Function of Time (C) Traction Torque and Wheel Speed as a Function of Time

Driving test around a large circle was done at a constant speed approximately. The direction of the driving was anticlockwise. The comparison of the two front wheels' performance follows, as shown in Figure 13. According to the vehicle dynamics, the response of the forces (F_x , F_y , F_z) and torque (M_y) of the right wheel should be larger than that of the left wheel, which can be seen from the curves clearly. More specifically, the vertical force (F_z) of the right wheel increases while that of the left wheel decreases relative to the static status, because the body of the vehicle will lean to the right side, as shown in Figure 13(c). The obvious change of the curves in the beginning is caused by the vehicle starting. Then the curves' value keeps at a stable level until braking. For the longitudinal force (F_x), although the increase of the vertical force (F_z) of the right wheel brings an increase of the motion resistance, but it also means a larger increase of the tractive force. Therefore, the response of the longitudinal force (F_x) of the two wheels is as shown in Figure 13(a). Figure 13(b) shows the result of the measurement of the lateral force, which can be used for the research of steering control and lateral stability. The lateral force of the right wheel has a larger increase than the left wheel. The driving torque (M_y) on the driving wheel is as shown in Figure 13(d). The obvious decrease in the middle of the curves is due to the driving behavior of releasing the accelerator to control the vehicle speed.



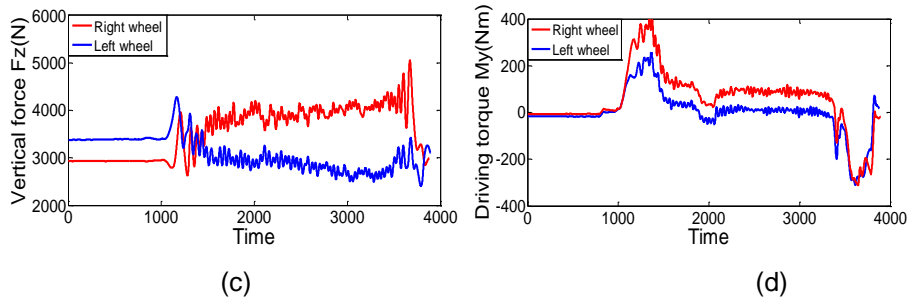


Figure 13. (a) Comparison of the longitudinal force of the two front wheels (b) Comparison of the lateral force of the two front wheels (c) Comparison of the vertical force of the two front wheels (d) Comparison of the traction torque of the two front wheels

In order to validate the capability of the WFT system further, Figure-8 driving was conducted at a constant speed approximately. In the first half of the test procedure, the vehicle drove anticlockwise. While in the second half, the vehicle drove clockwise. The dynamic responses of the forces (F_x , F_y , F_z , M_y) of the two front wheels are shown in Figure 14. When driving anticlockwise, the result reflected by the curves is similar to the situation in the circle driving. In the stage of driving clockwise, the whole situation is inversed, which is indicated by the comparison of the first half and the second half of all the curves. In particular, the value of the lateral force(F_y) changes from positive to negative because the lateral force is opposite to the positive direction ruled by the vehicle coordinate system when driving clockwise.

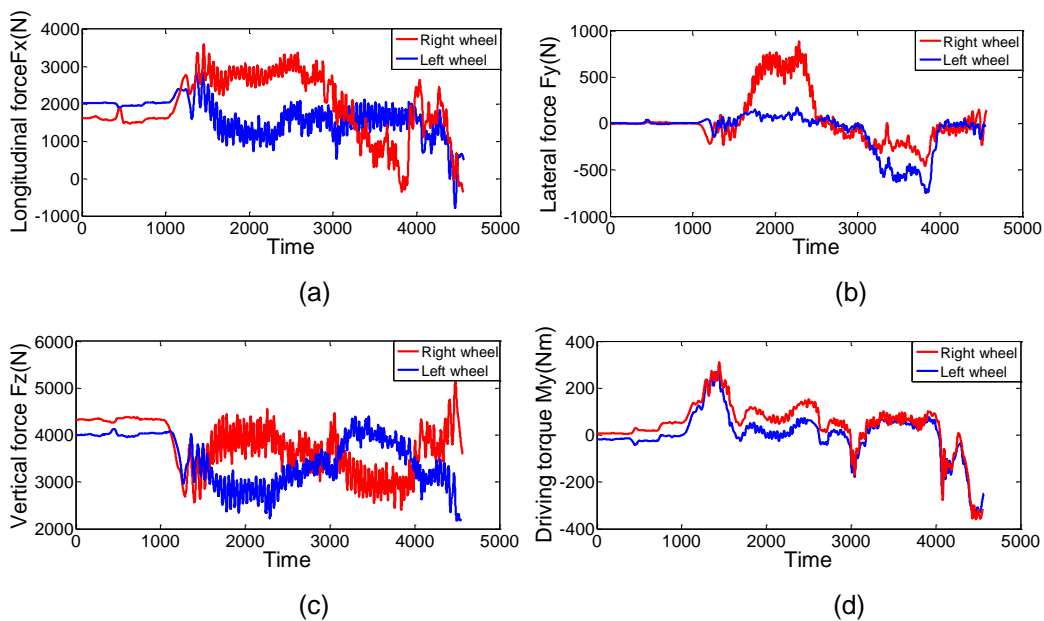


Figure 14. (a) Comparison of the longitudinal force of the two front wheels (b) Comparison of the lateral force of the two front wheels (c) Comparison of the vertical force of the two front wheels (d) Comparison of the traction torque of the two front wheels

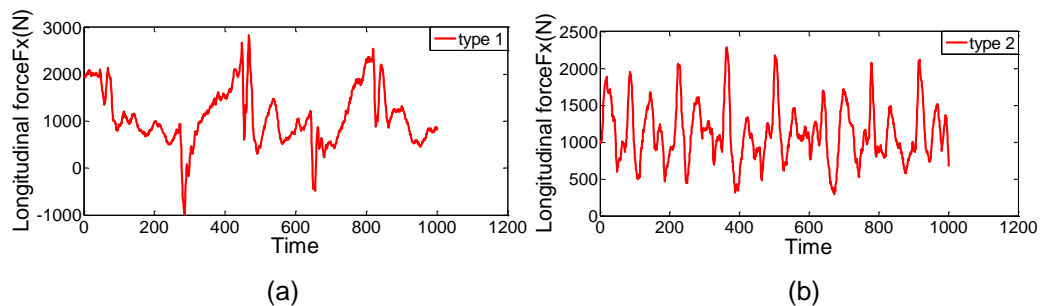
5.2. Off-Road Tests

In order to display the potency of the WFT system in off-road situations, the vehicle equipped with the WFT was tested on six kinds of special testing pavements, which were usually used for the vehicle durability test. As shown in Figure 15, they are the following roads: (1) twisted road; (2) concrete bump road; (3) discoid road; (4) washboard road; (5) gravel road; (6) Belgian road. The first three kinds of roads are too bumpy, so the vehicle drove slowly. For the next three kinds, the vehicle drove in three speed conditions: 10 Km/h, 20 Km/h and 30 Km/h.



Figure 15. Special Testing Pavements

In the attempt to show the potential of the WFT system in off-road situations, the longitudinal force (F_x) and the vertical force (F_z) are selected as the features of the response of the wheel-soil interaction. Fig. 16 shows the comparison of the longitudinal force (F_x) on six kinds of special testing pavements. Figure 17 shows the comparison of the vertical force (F_z). The value of each curve changes regularly, which validates the effectiveness and accuracy of the WFT system to some extent. There are obvious differences in the shape of the curves from each other, which indicate the different characteristics of the six kinds of special testing pavements. In particular, the gravel road and the Belgian road have the similar appearance to some extent. However, the curves of the longitudinal force and the vertical force both show significant distinction. Only a preliminary analysis is done here to show the potential of the WFT system. A further analysis of the curves will be done for specific research, such as terrain classification and loading-spectrum analysis.



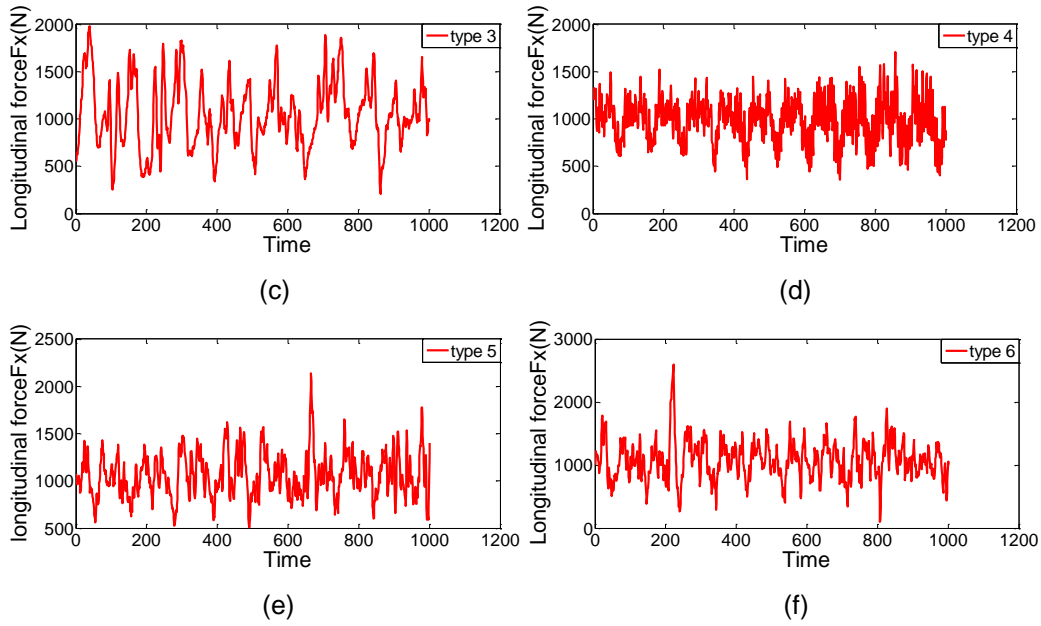


Figure 16. Comparison of the Longitudinal Force (Fx) On Six Kinds Of Roads

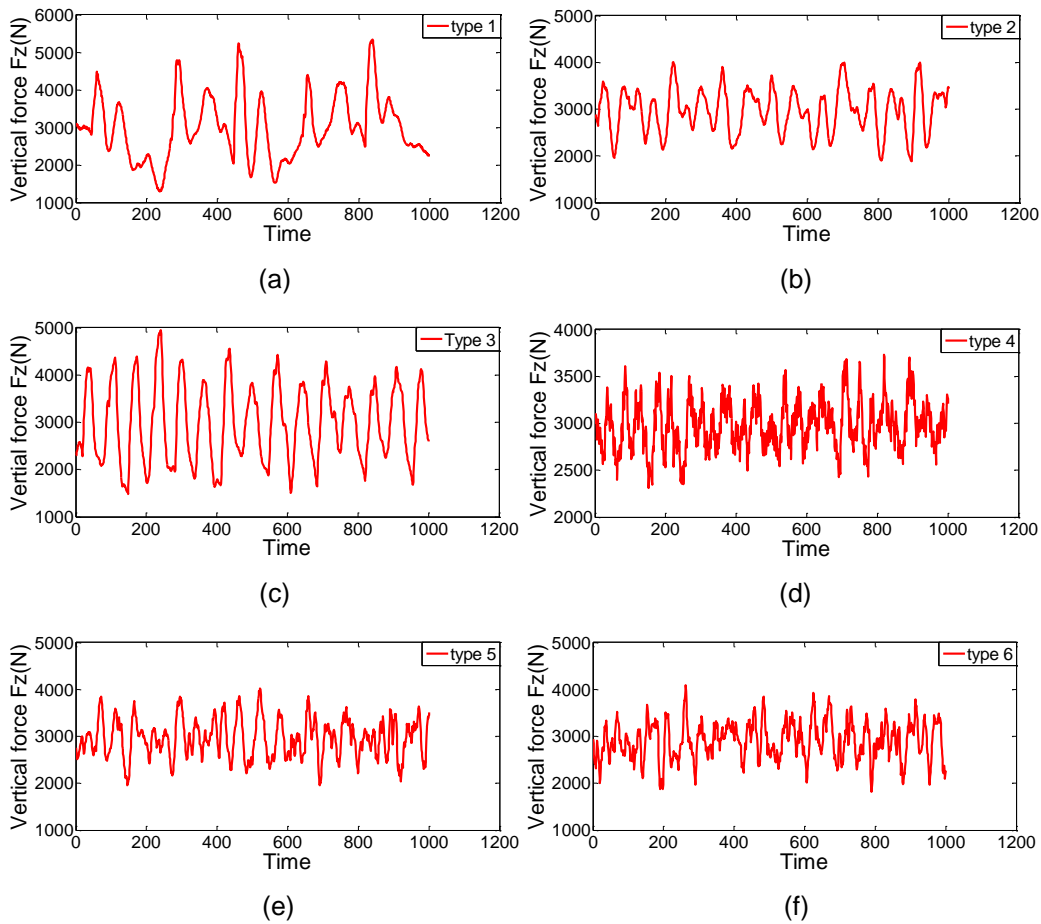


Figure 17. Comparison of the Vertical Force (Fz) on Six Kinds of Roads

6. Conclusions

A wheel force transducer (WFT) was designed and fabricated as a measuring instrument for off-road vehicle performance testing. The WFT has the function of measuring the forces and the torques synchronously and real-time. The overall structure of the WFT consists of several key parts: the sensor, the modified rims, the mounting parts and the automatic real-time data acquisition system. The elastomer of the sensor was designed with excellent mechanical strength and high sensitivity to fit the extreme working conditions caused by off-road situations. Minor modifications of the wheel rim were required for the application of the WFT, without any modification to the vehicle's structure. The installation of the WFT was convenient and only two persons can finish the work. The automatic real-time data acquisition system was designed through wireless transmission technology. The data of the WFT from different wheels can be acquired synchronously and real time, which provides the possibility of on-line analysis and real-time control of the vehicle. The results of the preliminary field tests are presented in the paper, which validates the validity, reliability and accuracy of the whole WFT system. Emphasis is lay on the analysis of the longitudinal force (F_x), the lateral force (F_y), the vertical force (F_z) and the driving torque (M_y) based on the driving maneuvers. The heeling torque (M_x) and the aligning torque (M_z) will be analyzed in further study. Then the results of off-road testing are presented. The longitudinal force (F_x) and the vertical force (F_z) are selected as the features of the response of the wheel-soil interaction. A sufficient expression is given to the different characteristics of the six kinds of special testing pavements by the results. A further analysis of the curves will be done for specific research. As a result, great potential of the WFT system is indicated in the application of off-road vehicle performance testing and wheel-soil interaction studies. Meanwhile, the cost of the WFT is controlled effectively under the condition of guaranteeing the reliability and accuracy of the whole system.

Acknowledgments

This work is supported by Natural Science Foundation of China (Grant no. 51305078) and Suzhou science and Technology Project (Grant no. SYG201303).

References

- [1] J.Y. Wong, "Theory of Ground vehicles, 4th edition", John Wiley & Sons, (2008).
- [2] C. Senatore and C. Sandu, "Off-road tire modeling and the multi-pass effect for vehicle dynamics simulation", Journal of Terramechanics, vol. 48, (2011), pp. 265-276.
- [3] Z. Shiller, M. P. Mann and D. Rubinstein, "Dynamic stability of off-road vehicle considering a longitudinal terramechanics mode", Roma, Italy 2007 IEEE International Conference on Robotics and Automation, (2007) April 10-14.
- [4] J. Pytka, "Experimental research on stability of an off-road vehicle on deformable surface", SAE Technical paper Series, (2010), 2010-01-1898.
- [5] J. Pytka, "Steering effects upon lateral dynamics of a SUV on deformable surfaces", SAE Int. J. Commer. Veh. vol. 4, no. 1, (2011), pp. 40-48.
- [6] V.V. Vantsevich, M. S. Vysotski and D. A. Doubovik, "Control of the wheel driving forces as the basis for controlling off-road vehicle dynamics", SAE Technical paper Series, (2002), 2002-01-1472.
- [7] V. K. Tiwari, K. P. Pandey and P. K. Pranav, "A review on traction prediction equations", Journal of Terramechanics, vol. 47, (2010), pp. 191-199.
- [8] M. G. Bekker, "Theory of Land Locomotion", Ann Arbor, The University of Michigan Press, (1956).
- [9] M. G. Bekker, "Introduction to Terrain-Vehicle System", Ann Arbor, The University of Michigan Press, (1969).
- [10] J.Y. Wong, "Terramechanics and Off-road Vehicle", Amsterdam, Elsevier, (1989).
- [11] J. D. Priddy and W. E. Willoughby, "Clarification of vehicle cone index with reference to mean maximum pressure", Journal of Terramechanic, vol. 43, (2006), pp. 85-96.
- [12] C. W. Fervers, "Improved FEM simulation model for tire-soil simulation", Journal of Terramechanics, vol. 41, (2004), pp. 87-100.

- [13] L.R. Khot, V. M. Salokhe, H. P. W. Jayasuriya and H. Nakashima, "Experimental validation of distinct element simulation for dynamic wheel-soil interaction", *Journal of Terramechanics*, vol. 44, (2007), pp. 429-437.
- [14] G. Ishigami, A. Miwa, K. Nagatani, K. Yoshida, "Terramechanics-Based Model for Steering Maneuver of Planetary Exploration Rovers on Loose Soil", *Journal of Field Robotics*, vol. 24, no. 3, (2007), pp. 233-250.
- [15] L. Ding, K. Yoshida, K. Nagatani, H. B. Gao, Z.Q. Deng, "Parameter Identification for Planetary Soil Based on a Decoupled Analytical Wheel-Soil Interaction Terramechanics Model", *The 2009 IEEE/RSJ International Conference on Intelligent Robots and Systems*, St. Louis, USA, (2009)October 11-15
- [16] K. Nagaoka, N. Mizukami, T. Kubota, "Prediction of Tractive Limitations of a Rigid Wheel on Loose Soil", *Journal of Asian Electric Vehicles*, vol. 10, no. 1, (2012), pp. 1583-1589.
- [17] W. Weiblen, H. Kockelmann and H. Burkard, "Evaluation of different designs of wheel force transducers", *SAE Paper*, (1999), 1999-00-1037.
- [18] J. Pytka, "A wheel dynamometer for off-road vehicles testing", *SAE Technical paper Series*, (2008), 2008-01-0783.
- [19] J. H. Lee, T. H. Johnson, D. Huang, S. Meurer, A. A. Reid and B. R. Meldrum, "New integrated testing system for the validation of vehicle snow interaction models", *Proceedings of the 2010 ground vehicle systems engineering and technology symposium*, (2010)August 17-19, Dearborn, Michigan.
- [20] G. Y. Lin, W. G. Zhang, F. Yang, H. Pang and D. Wang, "An initial value calibration method for the wheel force transducer based on memetic optimization framework", *Mathematical Problem in Engineering*, (2013), no. 275060.
- [21] D. Wang, G. Y. Lin, W. G. Zhang, N. Zhao and H. Pang, "The new method of initial calibration with the wheel force transducer", *Sensor Review*, vol. 34, no. 1, (2014), pp. 98-109.

Authors



Fan Yang, he was born in JiangSu province, China on June 1988. He is a Ph.D candidate in School of Instrument Science and Engineering, Southeast University. He is mainly engaged in research of Terramechanics, measurement and control technology.



Guoyu Lin, he was born in Fujian province, China on July 1979. He is an associate professor in School of Instrument Science and Engineering, Southeast University. His main research interests automotive, vehicle initiative safety and visual perception.



Weigong Zhang, he was born in Hangzhou province, China on October 1959. He is a professor and PhD supervisor in School of Instrument Science and Engineering, Southeast University. His main research interests automotive, vehicle initiative safety, measurement and control technology.

